

## Supporting Information

### **An Intrinsically Safe Gel Polymer Electrolyte Comprising Flame Retarding**

### **Polymer Matrix for Lithium Ion Battery Application**

*Hao Jia, Hitoshi Onishi, Ralf Wagner, Martin Winter\*, and Isidora Cekic-Laskovic\**

Hao Jia, Email: [jia@uni-muenster.de](mailto:jia@uni-muenster.de)

Dr. Ralf Wagner, Email: [ralf.wagner@uni-muenster.de](mailto:ralf.wagner@uni-muenster.de)

**Affiliation:** MEET Battery Research Center, University of Münster, Corrensstraße 46,  
48149 Münster, Germany

Hitoshi Onishi, Email: [Hitoshi.Onishi@mitsuichemicals.com](mailto:Hitoshi.Onishi@mitsuichemicals.com)

**Affiliation:** Mitsui Chemicals, Inc., 580-32 Nagaura, Sodegaura, Chiba 299-0265, Japan

Prof. Dr. Martin Winter (co-corresponding author), Email: [m.winter@fz-juelich.de](mailto:m.winter@fz-juelich.de)

Dr. Isidora Cekic-Laskovic (corresponding author), Email: [i.cekic-laskovic@fz-juelich.de](mailto:i.cekic-laskovic@fz-juelich.de)

**Affiliation:** Forschungszentrum Jülich GmbH Helmholtz-Institute Münster,  
Corrensstrasse 46, 48149 Münster, Germany

The supplementary information includes the detailed procedures of the polymer synthesis and preparation, the physicochemical properties of the polymer matrices, the comparative DSC studies and supplementary electrochemical performance characterization of NMC532/graphite cells comprising selected GPEs.

### Synthesis of dimethyl-p-vinyl benzyl phosphonate (DMpVBnP)

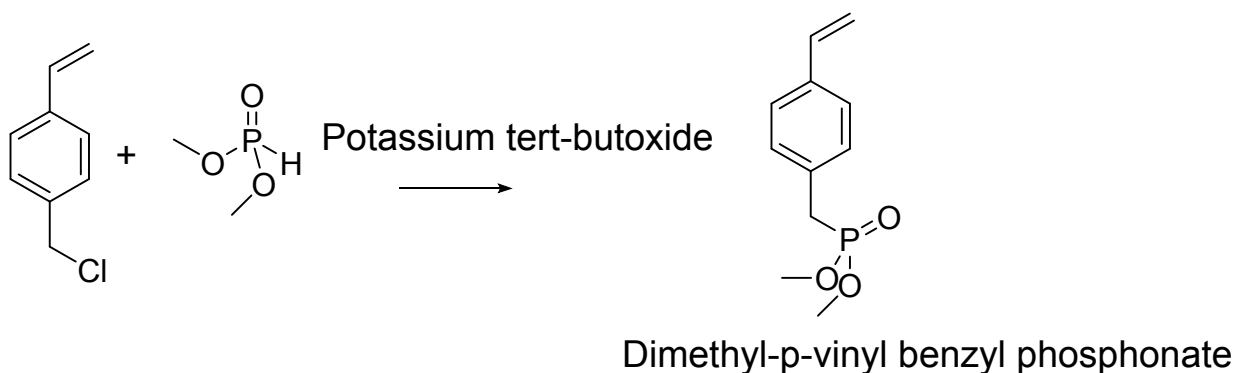


**Figure S 1.** Synthesis route of dimethyl-p-vinyl benzyl phosphonate

20 mL anhydrous oxolane (THF), 11 mL dimethyl phosphite (Sigma Aldrich, 98.0%) and 10 mL p-vinylbenzyl chloride (Sigma Aldrich, 90.0%) were introduced into a round bottom flask being constantly flushed with Ar. The solution of 8.16 g potassium tert-butoxide (Sigma Aldrich, 98.0%) in 20 mL anhydrous THF was slowly added into the flask within a period of 2h under cooling. After one hour of reaction, the obtained orange slurry was filtered. The liquid phase was diluted with 200 mL diethyl ether (Fisher Chemical, 99.5%) and washed with 100 mL deionized water for 3 times. The organic phase was separated and dried with MgSO<sub>4</sub> (Grüssing GmbH, 99.0%). Diethyl ether was thereafter removed by a rotary evaporator (Büchi®, Rotavapor® R-210) to yield the green yellowish crude product (9.7 g, yield= 71%, based on p-vinylbenzyl chloride). The crude product was then purified by column chromatography (ethyl acetate:acetone = 9:1 by vol. as eluent, R<sub>f</sub>= 0.40). After

the removal of eluent, the fine product (a colorless viscous oil) was obtained (yield= 48%, based on p-vinylbenzyl chloride).

**$^1\text{H}$  and  $^{31}\text{P}$  NMR spectra of the obtained DMpVBnP is presented below**

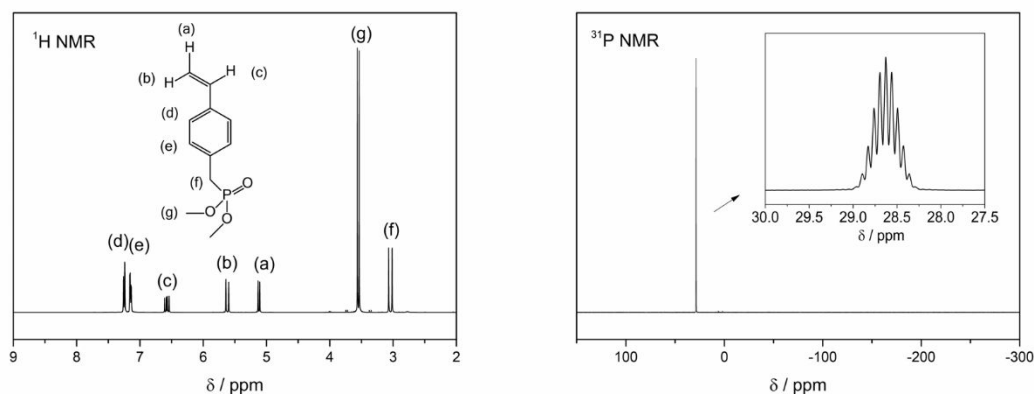


**Figure S 2.**  $^1\text{H}$  and  $^{31}\text{P}$  NMR of synthesized dimethyl-p-vinyl benzyl phosphonate

As shown in **Figure S 2**, no impurity peaks can be observed, indicating the high purity of the synthesized DMpVBnP monomer.

Synthesis of poly [dimethyl-p-vinyl benzyl phosphonate-co- oligo(ethylene glycol) methyl ether methacrylate] (c-PPO)

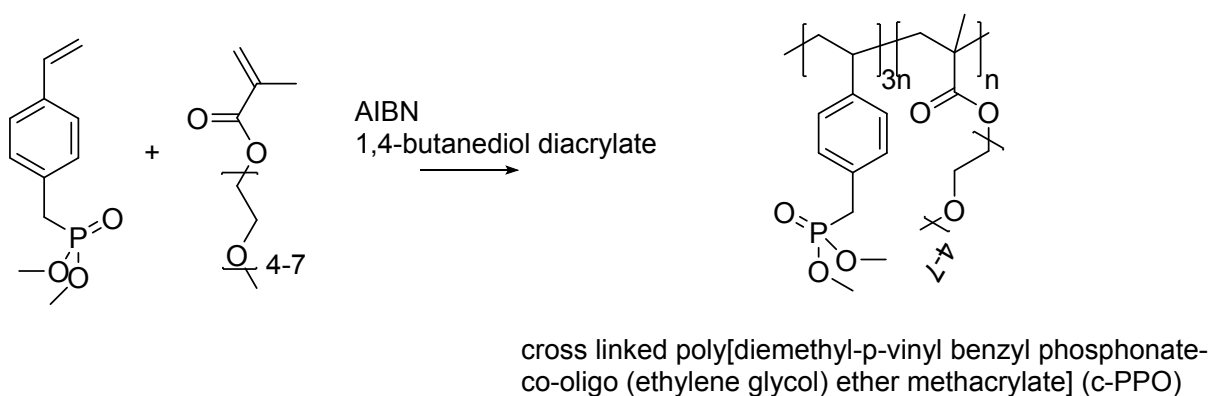


**Figure S 3.** Synthesis route of poly [diethyl-p-vinyl benzyl phosphonate-co-oligo (ethylene glycol) ether methacrylate]

Dimethyl-p-vinyl benzyl phosphonate (DMpVBnP), oligo (ethylene glycol) ether methacrylate (Sigma Aldrich, Average  $M_n=300 \text{ g mol}^{-1}$ ) were mixed at the molar ratio of 3:1. 0.1 wt. % of azobisisobutyronitrile (AIBN) and 2.0 wt. % of 1,4-butanediol diacrylate were introduced as the initiator and crosslinking agent, respectively. The obtained mixture was injected in a homemade template, comprised of a square frame shaped double side sticky tape sandwiched by 2 pieces of Mylar foil. The template was heated to  $70^\circ\text{C}$  for 12h. The obtained polymer membrane, was dried under reduced pressure ( $<10^{-3} \text{ mbar}$ ) at  $80^\circ\text{C}$  for 24 h to remove unreacted monomers. The dried polymer c-PPO was obtained as a transparent membrane with a thickness of  $200 \mu\text{m}$ .

**Synthesis of poly [benzyl methacrylate-co-oligo(ethylene glycol) methyl ether methacrylate] (PBO)**

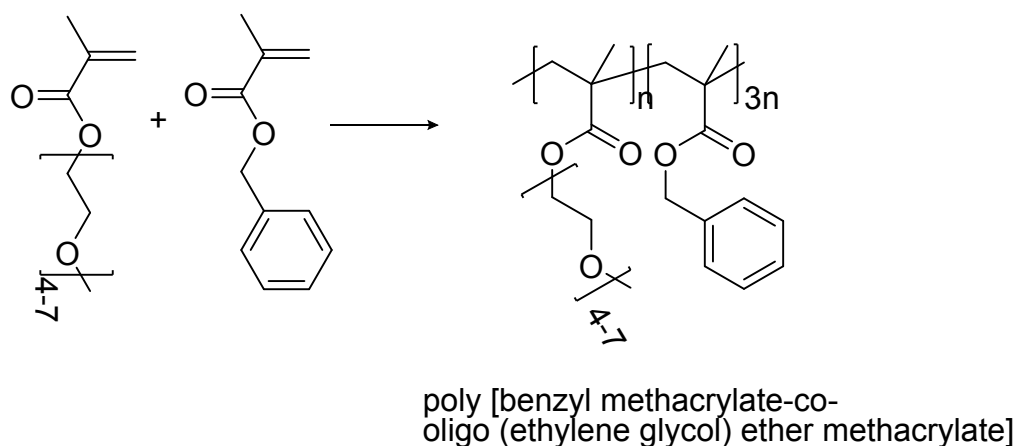


**Figure S 4.** Synthesis route of poly [benzyl methacrylate-co-oligo (ethylene glycol) ether methacrylate]

The synthesis of poly [benzyl methacrylate-co-oligo (ethylene glycol) methyl ether methacrylate] (PBO) was conducted according to the literature.<sup>1</sup> The precursor for the polymerization was comprised of the monomer mixture of benzyl methacrylate (BnMA) (Sigma Aldrich, 96%) : oligo(ethylene glycol) methyl ether methacrylate (OEGEMA) (Sigma Aldrich,  $M_n = 300 \text{ g mol}^{-1}$ ) = 3:1 by molar, and 0.2 wt. % of benzophenone as the initiator. The precursor was injected into the homemade template. The template was radiated with ultraviolet light (UVACUBE 100, Hönle AG) for 1 h. The obtained polymer membrane was dried at 100 °C under reduced pressure ( $<10^{-3}$  mbar) for 12 h to remove the unreacted monomers.

**FT-IR spectra of OEGMA, BnMA and PBO were depicted in Figure S 5**

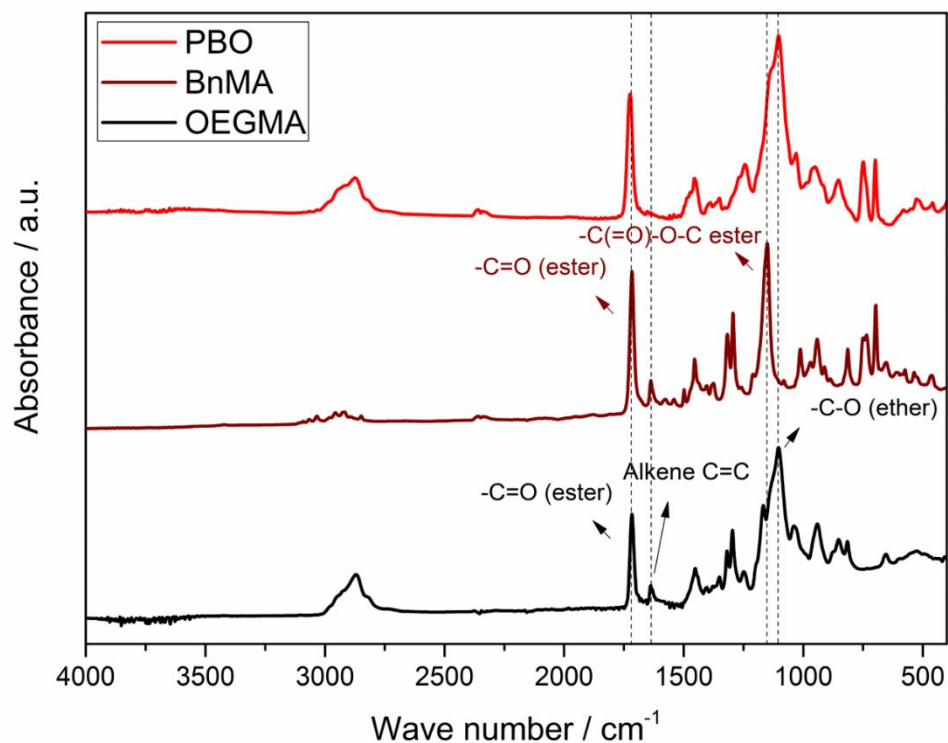


**Figure S 5.** Structural characterizations of PBO polymer matrix by the means of infrared spectroscopy

As shown in the graph, the peak ascribed to alkene disappeared after the polymerization. All the other characteristic peaks in the monomers can be identified in the co-polymer spectrum, indicating the successful synthesis of PBO.

### Preparation of porous PVDF-HFP membrane

PVdF-HFP (Kynar Flex® LBG), acetone (Fisher Chemical) and deionized water were mixed at the weight ratio of 1:8:1 in a sealed glass bottle. The bottle was thereafter heated up to 70 °C until a homogeneous solution was obtained. The solution was casted on a clean glass plate with a

doctor blade (gap width: 600  $\mu\text{m}$ ). After evaporating the acetone and water under ambient temperature overnight, the obtained polymer membrane was punched into  $\phi 16$  mm disks and further dried under reduced pressure ( $<10^{-3}$  mbar) at 60  $^{\circ}\text{C}$  for 12 h.

### Porosity of selected polymers determined by mercury porosimetry

The porosities of selected polymers are determined by mercury porosimetry. In the case of PVDF-HFP, the specific total pore volume is determined as 2.34  $\text{mL g}^{-1}$  at  $2 \times 10^6$  Pa. The specific volume of PVDF-HFP is 0.56  $\text{mL g}^{-1}$  (calculated by the density of 1.78  $\text{g mL}^{-1}$ ). The porosity of PVDF-HFP can be calculated by the following equation:

$$p = \frac{V_p}{V_p + V_{\text{polymer}}}$$

p: porosity;

$V_p$ : specific total pore volume;

$V_{\text{polymer}}$ : specific polymer volume;

The porosity of PVDF-HFP is determined as 80.6%. Similarly, the porosities of PBO and c-PPO were evaluated by mercury porosimetry. However,  $V_p$  are negligible in both cases of PBO (0.004  $\text{mL g}^{-1}$  at  $2 \times 10^6$  Pa) and c-PPO (0.020  $\text{mL g}^{-1}$  at  $2 \times 10^6$  Pa). For this reason, c-PPO and PBO can be regarded as non-porous polymers.

### Summary of physicochemical properties of the selected polymers

**Table S 1.** Physicochemical properties of the selected polymers

Polymer matrix	Thickness / $\mu\text{m}$	Liquid uptake ratio / %	Porosity / %
----------------	---------------------------	-------------------------	--------------

---

PVDF-HFP	$\approx 100$	480 wt. %	80.6
PBO	$\approx 200$	460 wt. %	0.0
c-PPO	$\approx 200$	210 wt. %	0.0

---

Due to the differences in nature between PVDF-HFP on one side and c-PPO and PBO on the other side, influencing the mechanical stability polymer matrices, the thickness of 100  $\mu\text{m}$  for c-PPO and PBO matrices is not sufficient to provide effective performance of the considered cell chemistry.

#### **DSC of cell components conducted by sealed pans**

TA Instrument Q2000 was employed to study the DSC of each cell component. Al pans are used for sealing the PVDF-HFP polymer matrix, the fresh NMC532 electrode and the fresh graphite electrodes. The DSC of LP30 electrolyte was conducted with a sealed pressure pan. The temperature increased from 30 to 250  $^{\circ}\text{C}$  at the rate of 5 $^{\circ}\text{C min}^{-1}$ .



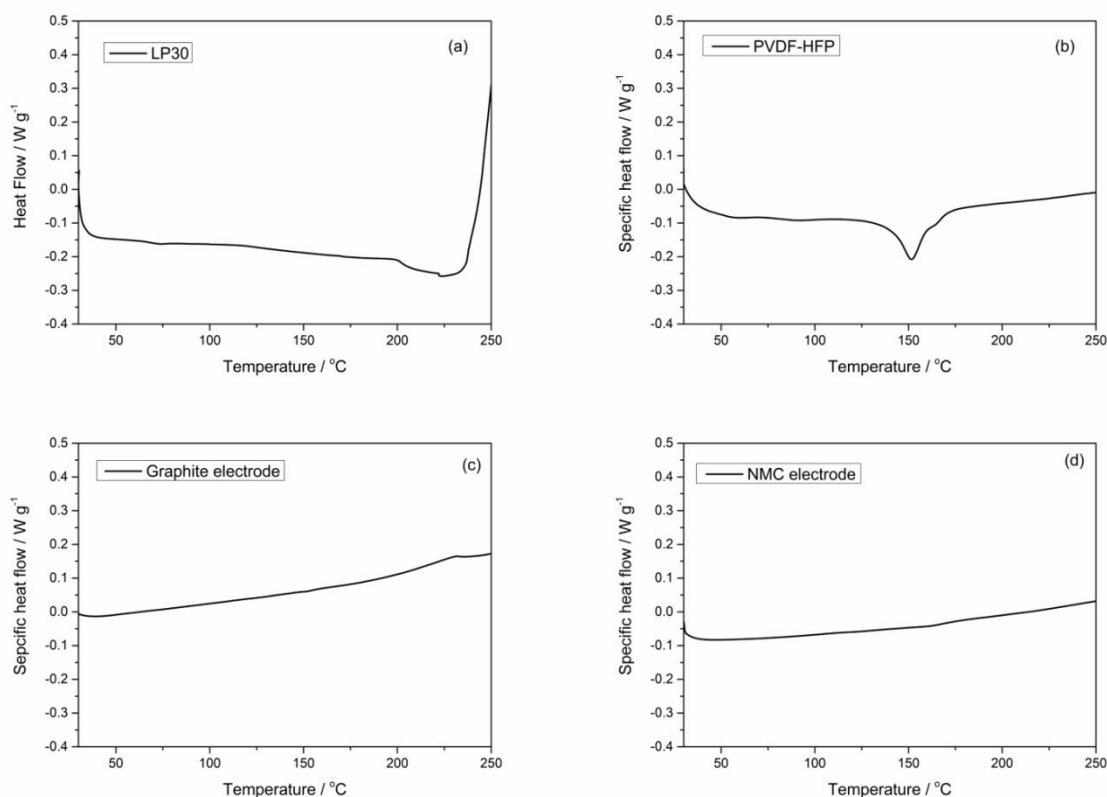


**Figure S 6.** Temperature dependent specific heat flow of cell components measured with sealed pans by DSC, (a) LP30 electrolyte, (b) PVDF-HFP polymer matrix, (c) fresh graphite electrode and (d) fresh NMC532 electrode

As shown in in **Figure S 6(b, c and d)**, no apparent exothermic reactions can be observed in the cases of PVDF-HFP polymer matrix, fresh graphite electrode and fresh NMC532 electrode in the temperature range from 30 to 250 °C. A weak endothermic peak could be observed in the case of PVDF-HFP at  $\approx 150$  °C, which could be assigned to the melting of PVDF-HFP. In the case of LP30 electrolyte, the decomposition of the electrolyte starts at  $\approx 230$  °C.

### DSC conducted by coin cells

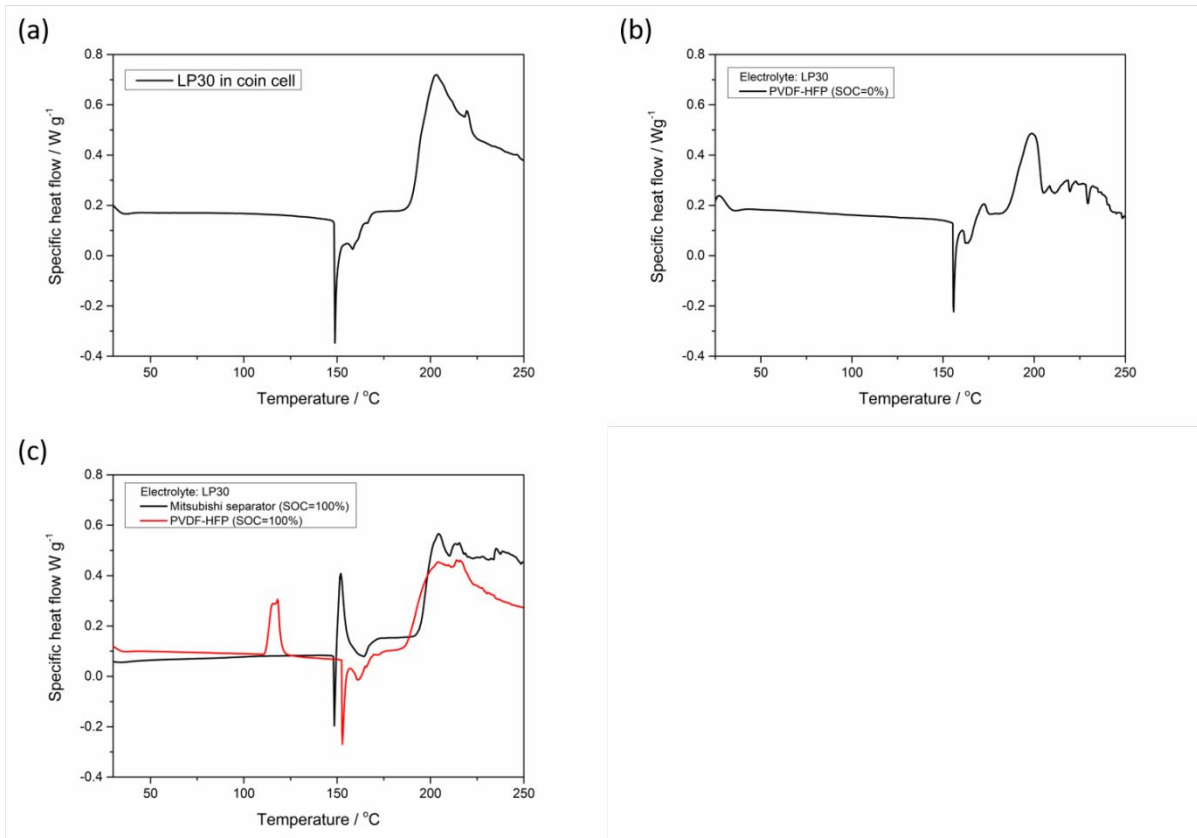


**Figure S 7.** Temperature dependent specific heat flow of liquid electrolyte or LIBs measured with coin cells by DSC

**Figure S 7 (a)** depicts the DSC curves of LP30 electrolyte in a coin cell. Compared with the DSC curves conducted with a pressure pan (**Figure S 7 (a)**), an extra sharp endothermic peak could be observed at  $\approx 150$  °C in DSC conducted with coin cell. After the DSC measurement conducted in coin cell, the casing of the coin cell comprising LP30 is ruptured. The rapid solvent evaporation after the rupture of the cell casing results in this sharp endothermic peak in the coin cell DSC.

**Figure S 7 (b)** shows then DSC of a freshly assembled NMC532/graphite LIB coin cells with PVDF-HFP/LP30 GPE. By comparing **Figure S 7 (a)** and **Figure S 7 (b)**, it can be concluded that the freshly assembled cell is very similar to the coin cell that contains only LP30, *i.e.*, the cell

components other than LP30 electrolyte can be regarded as inert in the case of freshly assembled cell.

**Figure S 7 (c)** shows the DSC curves of fully charged NMC532/graphite LIB coin cells with PVDF-HFP/LP30 GPE and separator/LP30 electrolyte. By comparing **Figure S 7 (b)** and **Figure S 7 (c)**, an exothermic peak at  $\approx 110$  °C can be observed in the fully charge cell comprising PVDF-HFP/LP30 GPE, which is absent in the case of freshly assembled cell. After substituting PVDF-HFP with a commercially available separator (Mistubishi separator NanoBaseX OZ-S30), this peak can no longer be observed, as shown in **Figure S 7 (c)**. In addition, as shown in the paper, this exothermic peak  $\approx 110$  °C is absent in the cases of cells comprising c-PPO and PBO based GPEs (**Figure 7 (b)** and **Figure 7 (c)**). All the evidences indicate that PVDF-HFP is the reason for this reaction, and this reaction only takes place in fully charged cell. As PVDF-HFP does not decompose at such temperature, it indicates that this peak originates from the interaction between the PVDF-HFP and other cell components. Combined with the studies reported in the literature, this reaction can be assigned to the reaction between PVDF-HFP and the lithiated graphite.<sup>2</sup>

A weak endothermic peak at  $\approx 160$  °C could be observed in all coin cells, which could be ascribed to the melting of the polypropylene sealing ring in the coin cell.

### **Conductivity and C-rate performance of NMC532/graphite cells comprising PVDF-HFP, PBO and c-PPO based GPEs**

The temperature dependent conductivity of the c-PPO/LP30 GPE was evaluated in a CR2032 coin cell setup including homemade ring-shaped plastic spacer. Two stainless steel disks were employed as the electrodes. As GPEs are flexible, the geometry of the GPE would change under mechanical pressure, leading to the variation of the cell constant. To keep the shape of the GPE fixed, a plastic ring (thicknesses:  $1 \times 100$   $\mu\text{m}$  for PVDF-HFP/LP30 GPE,  $2 \times 100$   $\mu\text{m}$  for c-PPO/LP30 GPE and

PBO/LP30 GPE) was applied to confine the GPE. The cell constant was determined as quotient of the thickness of the ring and the inner area of the ring. An oven (Binder MK 53) was employed to control the temperature. The temperature was increased stepwise from -15 to 60 °C in 5 °C steps. The conductivity cell was held at each temperature for 30 min prior to the impedance measurement. The electrochemical impedance spectra of the cells were measured with Solartron SI 1287 and Solartron 1260A impedance gain phase analysers. The frequencies of the input alternating voltage signals ranged from  $10^5$  to  $10^2$  Hz with an amplitude of 5 mV. The C-rate performance of NMC532/graphite cells comprising PVDF-HFP, PBO and c-PPO based GPEs was evaluated at 20 °C, under the C-rates of 0.1C, 0.2C, 0.5C, 1.0C, 2.0C, 5.0C and 10.0C.

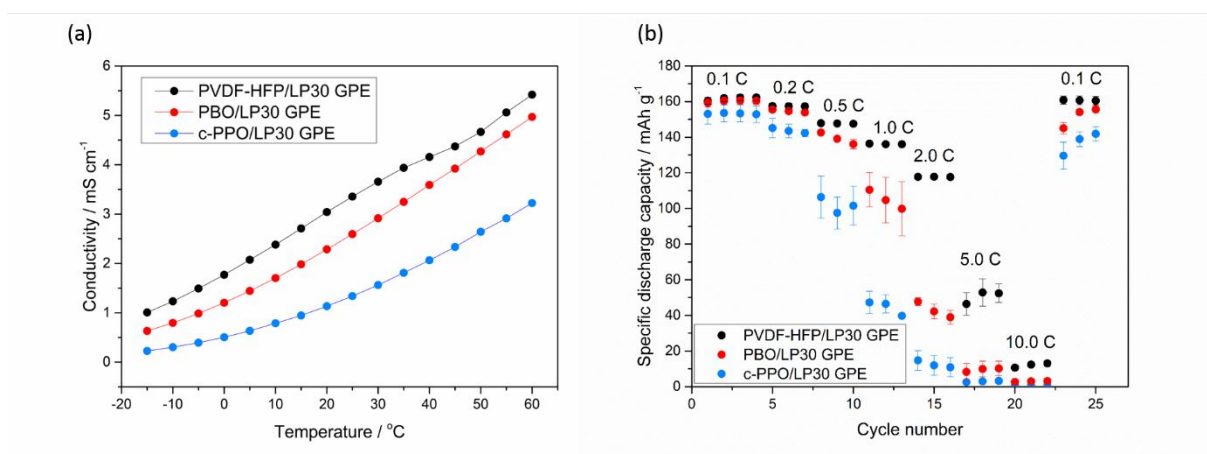


**Figure S 8.** (a) Dependence of conductivity of selected GPEs on temperature, (b) C-rate dependent specific discharge capacity of NMC532/graphite cells using selected GPEs

As illustrated in Figure S 8 (a), c-PPO/LP30 GPE shows the lower conductivity to the reference polymers. It can be assigned to the relatively low liquid electrolyte uptake ratio (210 wt. %) and the non-porous structure. Consequently, NMC532/graphite cells comprising the c-PPO/LP30 GPEs exhibit inferior C-rate performance to those comprising reference GPEs.

**Cycling performance comparison of cells using 1 mol L<sup>-1</sup> LiPF<sub>6</sub> in EC:DMC =1:1 by wt. (LP30) and 1 mol L<sup>-1</sup> LiPF<sub>6</sub> in EC:DMC:DMpVBnP=9:9:2 by wt.**

To illustrate the advantage of bonding DMpVBnP to the polymer matrix on the electrochemical performance of the LIBs, 10 wt.% DMpVBnP introduced in LP30 electrolyte as a miscible co-solvent. Therefore the formula of the DMpVBnP containing electrolyte is 1 mol L<sup>-1</sup> LiPF<sub>6</sub> in EC:DMC:DMpVBnP=9:9:2 (LPD for abbreviation).

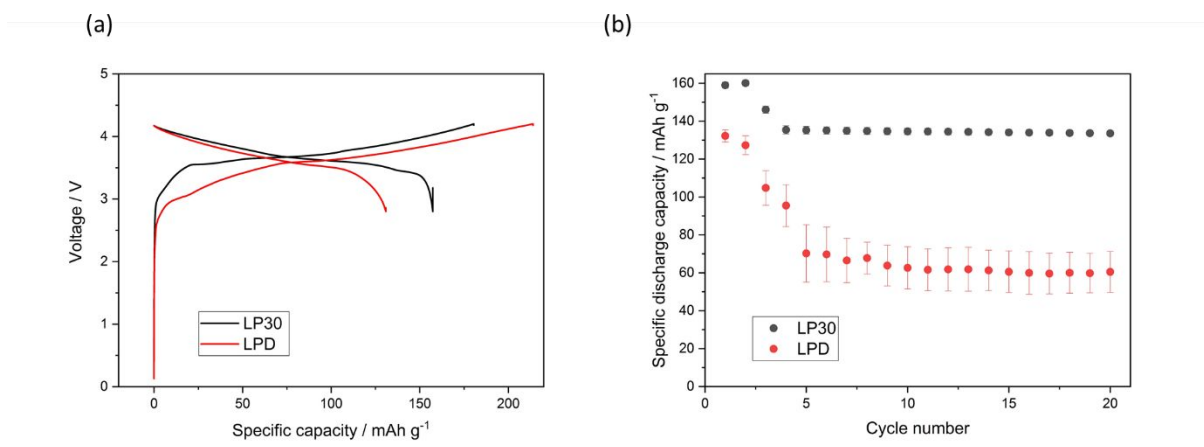


**Figure S 9.** (a) Voltage profile of NMC532/graphite cells comprising LP30 and LPD electrolytes plotted as the function of specific capacity in the first charge/discharge cycle at 0.1C; (b) cycling performance of NMC532/graphite cells comprising LP30 and LPD electrolytes.

As shown in **Figure S 9** (a), when DMpVBnP is directly introduced in the electrolyte, significant difference can be observed in the voltage-specific capacity profile of the first charge cycle, indicating that DMpVBnP participates in the faradic reactions of the formation cycles. The average Coulombic efficiency of the first cycle is 64.3 %, being significantly lower than that of the reference cells (87.3%). The introduction of DMpVBnP in liquid electrolyte induced significant irreversible capacity in the formation cycle. At 1.0C, the average specific capacity of the PVDF-HFP/LP30 GPE-based cells is 135 mAh g<sup>-1</sup>, whereas that of PVDF-HFP/LPD GPE-based cells is only 70 mAh g<sup>-1</sup>.

When being chemically bonded, no additional parasitic reactions can be observed even when DMpVBnP content reached 22 wt.% (**Figure 5**). In comparison, the DMpVBnP only amounts for 8 wt.% in PVDF-HFP/LPD GPE system, however, it has a significant detrimental effect on the electrochemical performance of the LIB. Since it is not immobilized by the chemical bonds, DMpVBnP can readily participate in the parasitic reactions at the electrode | electrolyte interphases and lead to deterioration of electrochemical performance of the LIBs.

## References:

- (1) Isken, P.; Winter, M.; Passerini, S.; Lex-Balducci, A. Methacrylate based gel polymer electrolyte for lithium-ion batteries. *Journal of Power Sources* **2013**, 225, 157-162.
- (2) Du Pasquier, A.; Disma, F.; Bowmer, T.; Gozdz, A.; Amatucci, G.; Tarascon, J. M. Differential Scanning Calorimetry Study of the Reactivity of Carbon Anodes in Plastic Li - Ion Batteries. *Journal of the Electrochemical Society* **1998**, 145 (2), 472-477.